ACS chemical biology

Articles

pubs.acs.org/acschemicalbiology

Structure-Guided Discovery of a Novel Aminoglycoside Conjugate Targeting HIV-1 RNA Viral Genome

Eric Ennifar,*[,†] Muhammad Waqar Aslam,[‡] Perrine Strasser,[†] Guillaume Hoffmann,[†] Philippe Dumas,[†] and Floris L. van Delft*[,‡]

[†]Architecture et Réactivité de l'ARN, Institut de Biologie Moléculaire et Cellulaire, CNRS, Université Louis Pasteur, 15 rue René Descartes, 67084 Strasbourg, France

[‡]Institute for Molecules and Materials, Radboud University Nijmegen, Heijendaalseweg 135, 6525 AJ, Nijmegen, The Netherlands

Supporting Information

ABSTRACT: The dimerization initiation site (DIS) of the HIV-1 genomic RNA is a conserved stem-loop that promotes viral genome dimerization by forming a loop-loop complex. The DIS constitutes a potentially interesting target because it is crucial for several key steps of the viral replication. In this work we describe the synthesis of a rationally designed aminoglycoside conjugate that binds the HIV-1 DIS viral RNA with high specificity, as shown by an extensive *in vitro* binding characterization. We propose a three-dimensional model of the drug−RNA interaction that perfectly fits with binding data. Our results show the feasibility of targeting the HIV DIS viral RNA dimer and open the way to the rationale design of a new class of antiviral drugs. In addition, due to similarities between the HIV-1 DIS RNA and the bacterial aminoacyl decoding site (A site) RNA, we show that this novel aminoglycoside conjugate also binds the bacterial A site with a similar affinity as natural aminoglycoside antibiotics.

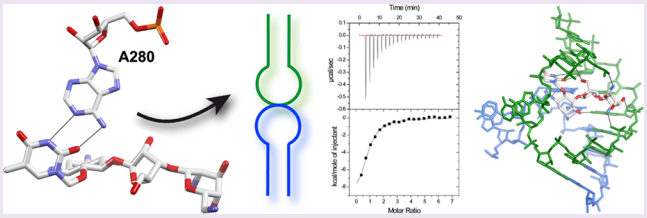

In the absence of a vaccine and in the context of increasing prevalence of resistant strains, identifying and validating new therapeutic targets and finding new inhibition strategies remain major goals of HIV research. Beside the viral proteins and cellular cofactors of HIV-1 replication, the genomic RNA itself has been proposed as an interesting target for antiviral agents. All retroviruses, including HIV-1, encapsidate their genome as a dimer of two single-stranded RNAs that are noncovalently linked close to their 5′-ends.[1] The HIV-1 dimerization initiation site (DIS) is a highly conserved sequence in the 5′ noncoding region of the viral genomic RNA.[2,3] It was shown that alteration of the DIS affects several key steps of the viral replication such as RNA dimerization, packaging, and reverse transcription and dramatically reduces viral infectivity, thus making the DIS a potentially interesting RNA target.[4,5] The DIS loop initiates genome dimerization by forming a loop−loop complex that is further stabilized into an extended duplex form upon interaction with the viral NCp7 nucleocapsid protein (Figure 1a).[6−9]

X-ray structures of the DIS kissing-loop complex and extended duplex forms[10−13] revealed surprising structural and sequence similarities with the bacterial 16 S rRNA aminoacyl-tRNA decoding site (A-site), which is the target of aminoglycoside antibiotics.[14,15] As a result, it was shown that 4,5-disubstituted 2-deoxystreptamine (2-DOS) aminoglycosides bind the "A site motif" within HIV-1 DIS *in vitro* with a high specificity and with a significantly higher affinity than their natural target, the bacterial A site.[16−20] Aminoglycoside binding to the viral RNA induces a strong stabilization of the DIS kissing-loop, thus interfering with its conversion into the extended duplex form.[16] Importantly, binding of aminoglycosides to the DIS was also observed on the complete viral genome *ex vivo* in HIV-infected human cells and in viral particles.[18] Crystal structures of DIS kissing-loop complex and extended duplex bound to several aminoglycosides were solved,[18,21] disclosing the molecular requirements for the drug/RNA recognition and opening the way to structure-based design of novel potential drugs.

Aminoglycoside antibiotics were among the first antibacterial agents active against both Gram-negative and Gram-positive pathogens and are currently still important for the treatment of some pathogens. Their interactions with the bacterial A-site RNA induce mRNA decoding errors, block mRNA and tRNA translocation, and inhibit ribosome recycling.[22−24] However, their relative toxicity and the rapid development of resistant strains prompted extensive research efforts in order to discover aminoglycoside derivatives with improved potency against resistant pathogens and reduced side effects.[25] In addition, intense research also focused on the development of novel aminoglycosides binding to new RNA targets, especially conserved and structured HIV-1 RNA sequences. Aminoglycoside dimers were thus developed to confer selectivity for the HIV-1 RRE (rev response element),[26] the TAR (trans-activation responsive element),[27,28] or the DIS.[29] The develop-

Received: July 5, 2013
Accepted: September 9, 2013

   dx.doi.org/10.1021/cb400498n | *ACS Chem. Biol.* XXXX, XXX, XXX−XXX

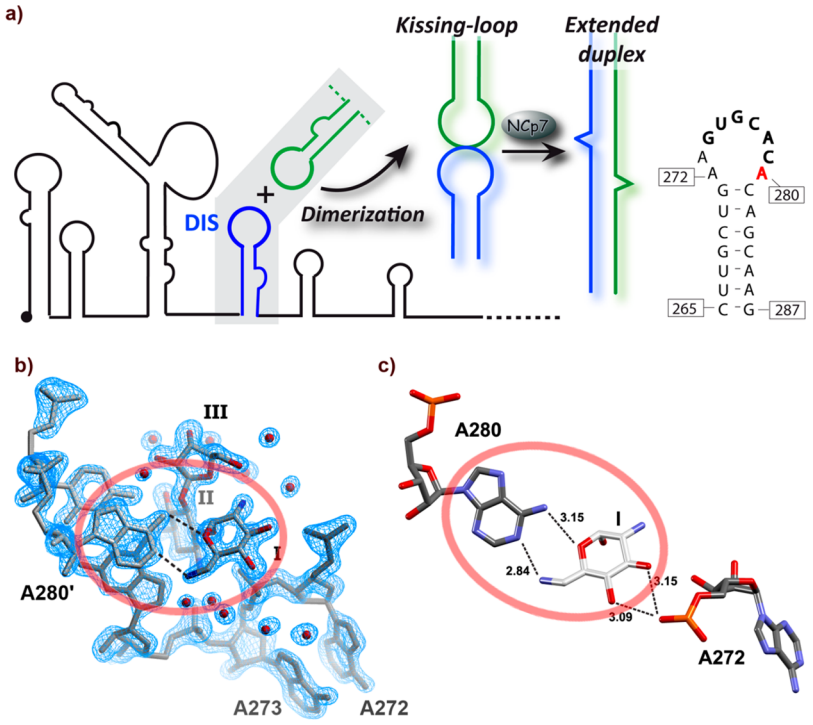

Figure 1. (a) HIV-1 genomic RNA dimerization mechanism and RNA sequence corresponding to the HIV-1 subtypes A and F used in this study. The self-complementary sequence is bolded, and the adenine 280 is highlighted in red. (b and c) Detailed views of the HIV-1 DIS-ribostamycin complexes showing the pseudo Watson−Crick base-pair. (b) DIS extended duplex crystal structure (PDB ID 3C3Z) superimposed with the electron density map. (c) DIS kissing-loop complex crystal structure (PDB ID 2FCZ).

ment of nucleobase-aminoglycoside conjugates was also explored to target the HIV-1 TAR.[30]

In this work, by combining previous structural and thermodynamic data about DIS/aminoglycoside complexes, we could rationally design and synthesize a nucleobase-aminoglycoside conjugate that targets the HIV-1 DIS RNA dimer. The specificity of the interaction was assessed by an extensive binding study based on isothermal titration calorimetry (ITC). Finally, we could show that our synthetic analogue also recognize *in vitro* the bacterial A-site with a similar affinity to that of natural aminoglycosides.

RESULTS AND DISCUSSION

Design and Synthesis of the Thymine-Neomycin Aminoglycoside Conjugate. Examination of all DIS/aminoglycoside crystal structures revealed that the highly conserved adenine 280 of the viral RNA genome is involved in a key interaction with ring I of aminoglycosides (Figure 1b,c). We therefore hypothesized that replacing ring I by a thymine nucleobase would lead to similar interactions, forming a Watson−Crick base-pairing between A280 and the drug, without significantly affecting the specificity and affinity of binding. Because neomycin was found to be the best DIS binder,[16] a neomycine-thymine conjugate was designed (compound **1**, Figure 2).

The synthesis of the envisaged thymine-neomycin conjugate **1** started with the commercially available neomycin B sulfate, which was transformed to fully protected peracetylated hexaazidoneomycin **2** [38] via transition metal catalyzed diazotransfer, followed by global O-acetylation. We argued that Lewis acid promoted fragmentation of the peracetylated hexaazidoneomycin **2**, as reported by Swayze,[39] followed by glycosylation of the resulting fragments after protective group

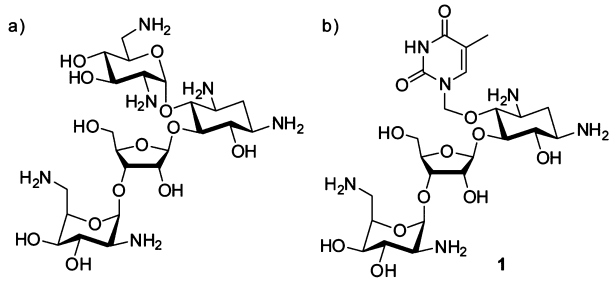

Figure 2. (a) Structure of neomycin. (b) Structure of thymine-neomycin conjugate **1**.

interconversion, would differentiate the two similar rings I and IV. Thus, compound **2** was treated with 3 equiv of $BF_3{\cdot}OEt_2$ and 1.1 equiv of *p*-CH_3PhSH (TolSH) in CH_2Cl_2 to yield 1,3,2′,6′-tetraazido-tri-*O*-acetyl-D-neamine **3** and per-*O*-acetyl-neobiosamine **4** (Scheme 1). Unfortunately, the R_f difference between compound **3** and **4** was too small to allow chromatographic separation, and therefore the crude mixture was treated with hexamethyldisilazane and catalytic TMSCl in CH_3CN to convert the free 5-OH of **3** to the more lipophilic TMS ether, followed by a facile separation step and acid hydrolysis of the TMS ether to afford the pure compound **3** in good yield. The resulting disaccharide **4** has the proper functionality at the ribose anomeric center for activation with thiophilic promoters and to allow glycosylation after protective group interconversion.

In the next step, per-*O*-acetyl-neobiosamine **4** was treated with KO^{t}Bu in MeOH to remove the acetyl groups, followed by conversion of the unprotected compound **5** into benzyl derivative **6** upon treatment with NaH and BnBr (Scheme 2). Next, glycosylation of **3** with thioglycoside donor **6** was

dx.doi.org/10.1021/cb400498n | *ACS Chem. Biol.* XXXX, XXX, XXX−XXX

Scheme 1[a]

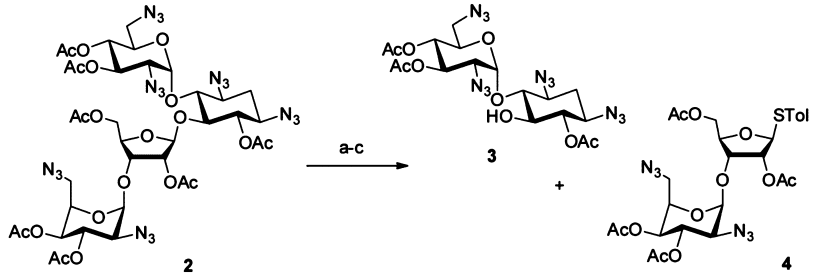

[a]Reagents and conditions: (a) TolSH (1.1 equiv), $BF_3{\cdot}OEt_2$ (3.0 equiv), CH_2Cl_2, rt, 15 h. (b) HMDS, TMSCl, CH_3CN, 3 h. (c) 1 M HCl, THF, rt, 30 min. (**3**, 82%; **4**, 74%).

Scheme 2[a]

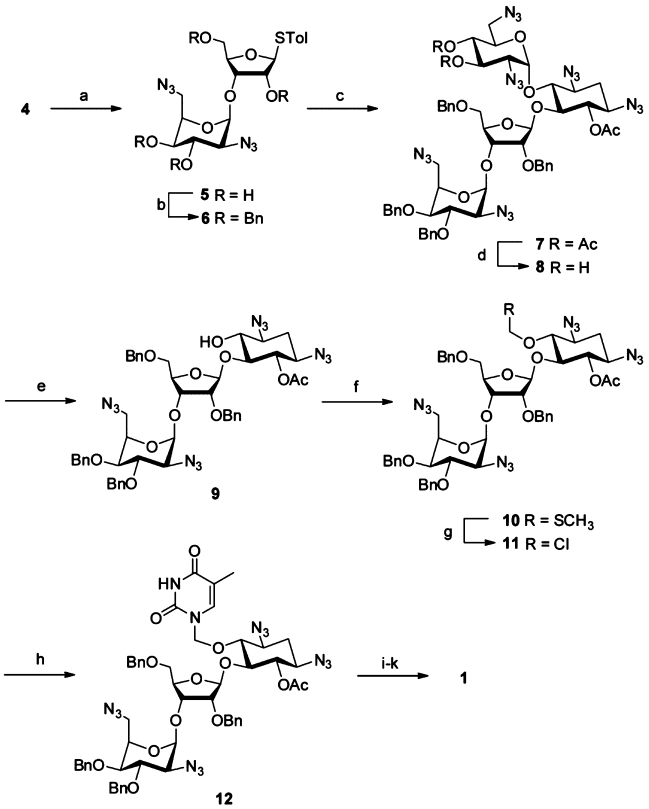

[a]Reagents and conditions: (a) KO^{t}Bu, MeOH, rt, 2 h (91%). (b) NaH, BnBr, DMF, 0 °C → rt, 3 h (83%). (c) **3**, NIS, AgOTf, CH_2Cl_2, MS 4 Å, −40 → −10 °C, 1 h (51%). (d) KO^{t}Bu, MeOH, rt, 2 h (65%). (e) (*i*) $NaIO_4$, MeOH, rt, 16 h. (*ii*) *n*-$BuNH_2$, MeOH, rt, 16 h (70% over two steps). (f) DMSO, Ac_2O, AcOH, 16 h (60%). (g) SO_2Cl_2, CH_2Cl_2, 1 h (70%). (h) 5-Methyl-2,4-bis(trimethylsilyloxy)-pyrimidine, *n*-Bu_4NI, $C_2H_4Cl_2$, 40 h, reflux (80%). (i) LiOH, MeOH, 1,4-dioxane, H_2O, 48 h (79%). (j) PMe_3, THF, 0.1 M NaOH, 4 h (84%). (k) $Pd(OH)_2$, H_2, AcOH, H_2O, 4 h (94%); TFA, MeOH.

attempted. After several attempts, it was found that NIS-promoted coupling of neamine acceptor **3** with thioglycoside donor **6** in CH_2Cl_2 gave the desired compound **7** in reasonable yield and with a favorable α/β ratio of approximately 1:6.5. Since it was found impossible to separate the anomers, we continued with the mixture of anomers with the objective to separate them at a later stage of the synthesis. The next target was to remove ring I of the resulting neomycin derivative **7** so thymine could be introduced at 4-OH. As anticipated, the selective deacetylation[40] of compound **7** with KO^{t}Bu in MeOH afforded monoacetate **8** in high yield. Oxidative cleavage of the unprotected diol functionality **8** with $NaIO_4$ in MeOH and subsequent elimination of the resulting dialdehyde proceeded uneventfully to yield pseudotrisaccharide **9** with the 4-OH free.

Finally, compound **9** was treated with DMSO, Ac_2O, and AcOH to produce the methyl thiomethyl ether **10**.[41] Reaction of compound **10** with SO_2Cl_2 in CH_2Cl_2 gave chlorinated compound **11**, which was refluxed overnight with bis-(trimethylsilyl)thymine and *n*-Bu_4NI in dichloroethane to afford the desired thymine-substituted derivative **12**. We then proceeded to remove all protecting groups. First, saponification of the acetyl ester of compound **12** was attempted under Zemplen conditions, but the acetyl group was found unaffected. After exploring a range of conditions, we succeeded in removing the acetyl group by treating compound **12** with LiOH in a mixture of H_2O and dioxane for 48 h. Next, azides were reduced by treating with PMe_3 in a mixture of THF and aqueous NaOH, and finally benzyl ethers were removed by hydrogenolysis in the presence of Pearlman's catalyst[42] in aqueous AcOH/MeOH, to afford fully deprotected thymine-substituted neomycin analogue **1** as the tetraacetic acid salt. For analytical purposes, acetate counterions were exchanged for trifluoroacetates by lyophilization from 2% TFA in MeOH.

Molecular Modeling of the Drug−RNA Interaction. Based on known HIV DIS RNA/neomycin structures, a 3D model of the DIS kissing-loop/compound **1** complex was built. Two molecules of compound **1** were placed in the DIS kissing-loop homodimer, similarly to the parent compound neomycin. This model shows that with a small accommodation of ring II, which was slightly rotated compared to the DIS/neomycin complex, all direct RNA/neomycin interactions involving rings II (the 2-DOS ring), III, and IV can be preserved by forming a Watson−Crick base-pairing between the thymine moiety of compound **1** and adenine 280 (Figures 3 and 4, Supplementary Figure 7). However, four direct contacts involving ring I of neomycin with phosphates 272 and 273 are lost due to the substitution into thymine (Figure 3). Interestingly, these four drug-phosphate RNA interactions are not present in the neomycin/ribosomal A site complex due to the difference in RNA topology between the A site and the HIV DIS kissing-loop. In addition, following accommodation of ring II, distances between N1, N3, and O6 and their respective RNA ligands slightly increased. Possible consequences of this distance change and loss of direct interactions will be discussed later. Regarding stacking interactions, an optimal stacking was observed in crystal structure between ring I of natural aminoglycosides and guanosine 271, but no stacking was observed with guanosine 274. The situation is different in the

dx.doi.org/10.1021/cb400498n | *ACS Chem. Biol.* XXXX, XXX, XXX−XXX

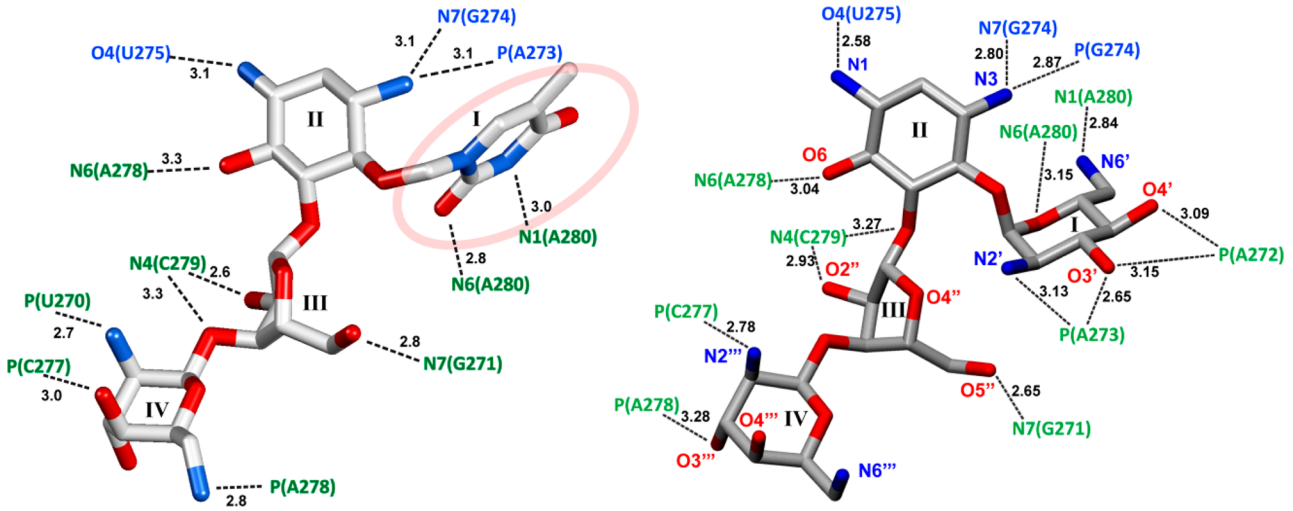

Figure 3. Comparison of predicted RNA–drug contacts for compound **1** (left) with observed RNA–neomycin interactions (PDB ID 2FCY, right). The thymine moiety is red-circled. Distances are indicated in angstroms. RNA ligands are indicated in green or blue depending on the strand to which they belong.

present model with compound **1**, likely because of the aforementioned obligatory accommodation and the rigidity of the thymine base in comparison of the flexible ring I. In the model, partial stacking interactions are expected both with guanosine 271 and guanosine 274 (Figure 4). These differences might also affect the affinity of compound **1** compared to that of neomycin.

***In Vitro* Binding Assay of Compound 1 to the HIV-1 DIS RNA Loop–Loop Complex.** The binding of compound **1** to the HIV-1 DIS kissing-loop RNA was then evaluated *in vitro* using isothermal titration calorimetry (ITC) on a 23-nucleotide fragment containing the minimal DIS hairpin loop (Figure 1a, Supplementary Figure 1). ITC is a true in-solution technique that directly measures the heat released or absorbed during a reaction, providing in one single experiment the complete binding profile (ΔH, ΔS, affinity constant, and stoichiometry) of this reaction. ITC experiments performed at 25 °C in the presence of 25 mM sodium cacodylate pH 7.0, 2 mM $MgCl_2$, and 100 mM KCl ("low salt" conditions) confirmed that, as predicted, compound **1** binds the DIS kissing-loop (Table 1) with a 2:1 stoichiometry (two ligands per DIS kissing-loop dimer). However, as anticipated from the model suggesting the loss of four direct drug/RNA hydrogen bonds and a nonoptimal stacking of the thymine moiety with the guanosine 271, the affinity is decreased compared to that of natural aminoglycosides (Supplementary Figures 2, 3, and 4). This decrease in affinity is also partly due to the loss of two amino groups (compared to the parent compound neomycin), which are mostly positively charged at pH 7.0 and therefore strongly contribute to affinity through electrostatic interactions.

In order to investigate the specificity of the binding, ITC experiments were then performed at higher salt concentration. In presence of 200 mM KCl ("high salt" conditions), unspecific interactions of paromomycin and lividomycin aminoglycosides with the DIS RNA are prevented (Supplementary Figure 5) but the specific binding is still preserved. Due to additional positively charged amino groups, unspecific interactions are still observed (but strongly reduced) with neomycin in these conditions (Supplementary Figures 4 and 5). In "high salts" conditions, compound **1** binds the DIS kissing-loop, and no unspecific interaction was detected (Figure 5). However, the binding occurs with a 7-fold loss in affinity (K_d = 5.3 μM) compared to "low salt" conditions. The specificity of binding was further assessed using various RNA sequences. No significant binding to compound **1** was detected by ITC on the ribosomal 23 S sarcin-ricin hairpin loop (SRL), which does not bind any aminoglycoside specifically, or on the HIV-1 TAR hairpin loop, which binds neomycin but in a different geometry not involving Watson–Crick-like base pairing with ring I,[43] or on a 22-base-pair duplex corresponding to the DIS sequence deprived of "A site motif" (Figure 5). Finally, the binding of compound **1** was also evaluated on a DIS A280U mutant sequence. This adenine to uridine mutation should disrupt the Watson–Crick hydrogen bonds between residue 280 and the thymine moiety of compound **1**. As expected, this sequence does not bind the neomycin-thymine conjugate (Figure 5). This clearly assesses the specificity of compound **1** binding to the HIV DIS dimer and the formation of the expected A-T base-pair between the drug of the viral RNA.

We have previously shown that DIS sequences with a $G_{274}CGCGC_{279}$ self-complementary sequence found in HIV subtype B are not able to interact specifically with aminoglycosides due to a steric hindrance between the amino group of C275 and N1 of ring II.[18,19] The binding of compound **1** to HIV-1 subtype B DIS kissing-loop was therefore also investigated. Surprisingly, ITC data revealed that compound **1** also interacts specifically with this DIS sequence both in low (Table 1) and high salt conditions (K_d = 5.6 μM), with an affinity very similar to the one observed for the subtype F DIS (Figure 5). Very likely, the binding is possible due to the slight obligatory accommodation of ring II in compound **1**, as previously mentioned, thus avoiding any steric hindrance between the RNA and the ligand. This observation is important since compound **1** is the first ligand that is able to bind indifferently any HIV DIS RNA dimer, thus circumventing the serious limitation of natural aminoglycosides, which could only bind DIS RNA having the $G_{274}UGCAC_{279}$ self-complementary sequence.

Interestingly, though binding affinities of compound **1** to HIV-1 DIS subtype F and B are similar, enthalpy and entropy changes are different in low salt conditions (Table 1). The origin of this enthalpy/entropy compensation is not obvious

dx.doi.org/10.1021/cb400498n | *ACS Chem. Biol.* XXXX, XXX, XXX–XXX

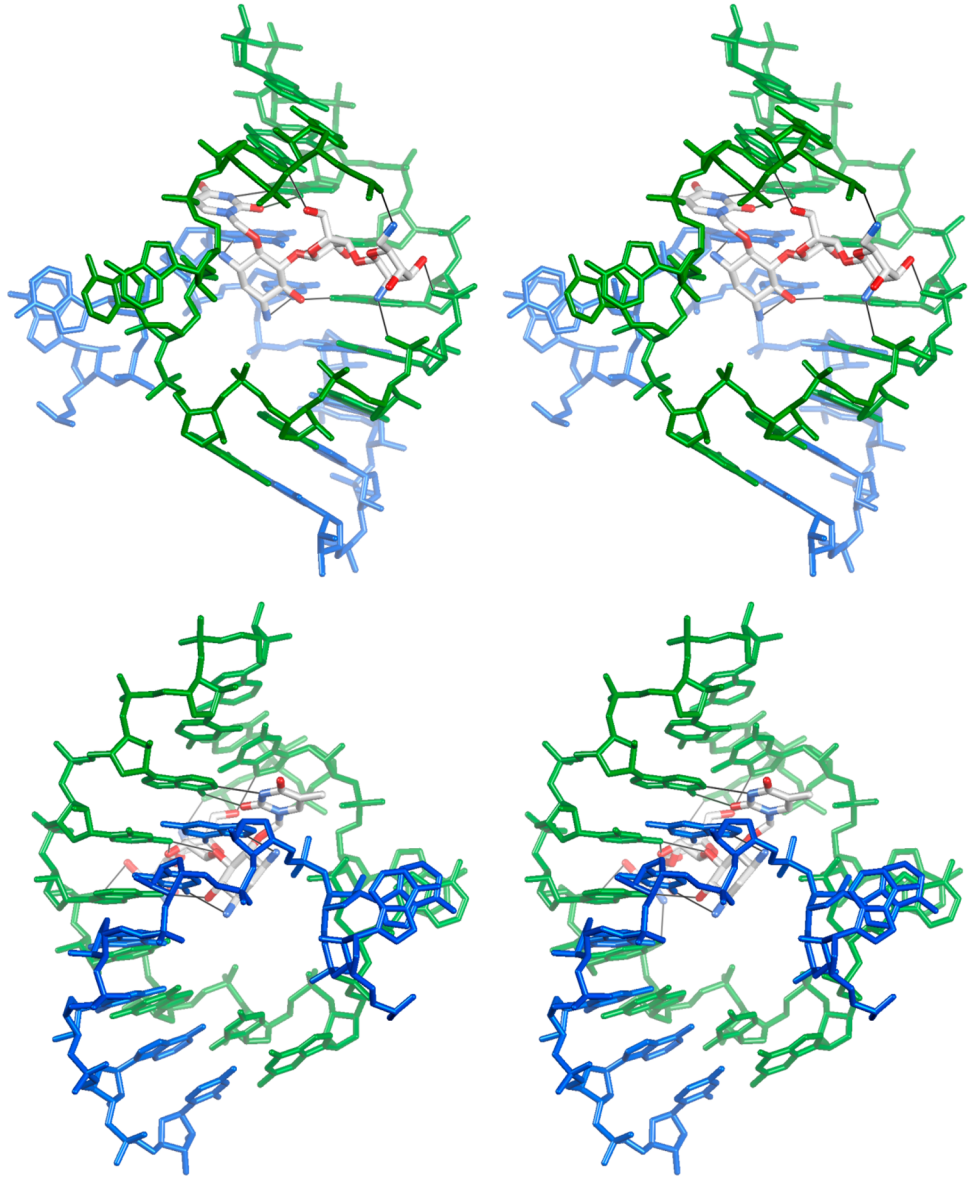

Figure 4. Two different stereo views (rotated by 180° along the RNA axis) of the 3D model of the HIV-1 DIS kissing-loop bound to compound **1**. The two RNA strands are shown in blue and green. Direct hydrogen bonds are depicted in dark gray.

Table 1. Binding Parameters Obtained by ITC Measurements for Compound 1 in Buffer Containing 100 mM KCl

RNA sequence	N^a	K_d (nM)	ΔH (kcal mol^{-1})	$-T\Delta S$ (kcal mol^{-1})
HIV DIS-F	0.96	730	−8.0	−0.5
HIV DIS-B	1.01	752	−13.6	5.0
bacterial A site	1.12	507	−7.2	−1.5

[a]Stoichiometry for one RNA strand.

from the model showing final bound state of drug/RNA interactions, since both complexes are expected to be almost identical. However, a major difference between both DIS subtypes is found in unbound structures: whereas a specific hexahydrated Mg^{2+} was found in crystal structures of the DIS subtype F loop−loop helix,[10] no cation was found in subtype B.[12] Consequently, displacement of a specific hexahydrated Mg^{2+} is a prerequisite for the binding of compound **1** to the subtype F DIS, but not to the subtype B DIS (disordered monovalent ions, instead of an ordered divalent cation, are likely displaced following ligand binding to this RNA sequence) and this could be the origin of the observed differences in ΔH and ΔS for these two RNA. Supporting this hypothesis, almost no difference in ΔH and ΔS are observed for ITC experiments performed in higher monovalent salt concentrations where Mg^{2+} cations might be partially screened by K^+ ions (Figure 5).

Binding of Compound 1 to the Bacterial Ribosomal A Site. Interactions between the bacterial A site and natural aminoglycosides have been extensively investigated using biophysical approaches,[15,44−52] resulting in the identification of modified aminoglycosides with improved binding properties.[53−58] Since the pseudo base-paring interaction between ring I and adenine 1408 of bacterial rRNA is also conserved in A site/aminoglycoside interactions,[15,45,51,52] we anticipated that compound **1** could also bind the bacterial A site *in vitro*. This interaction was therefore investigated by ITC on a 27-nucleotide RNA fragment containing the bacterial A site.[59] As expected, a specific 1:1 binding was observed (Table 1), but

dx.doi.org/10.1021/cb400498n | *ACS Chem. Biol.* XXXX, XXX, XXX−XXX

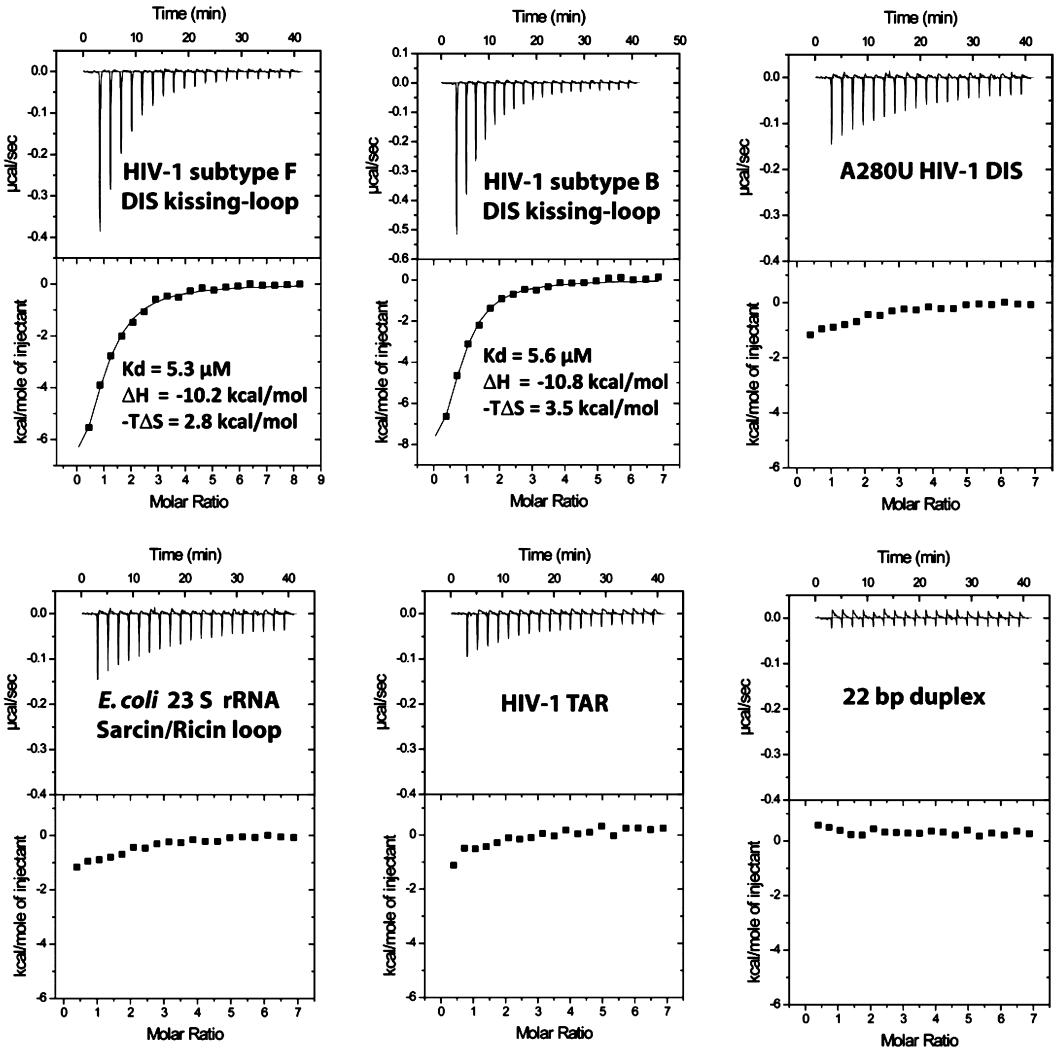

Figure 5. Isothermal titration calorimetry experiments showing the specific binding of compound **1** to the DIS kissing-loops from HIV-1 subtypes F and B. The binding is lost by mutating the adenine 280, which should interact with the thymine moiety, into uridine. No binding is observed on a 22 base-pair duplex, the ribosomal SRL hairpin loop or on the HIV-1 TAR loop.

again with a slight decrease in affinity compared to natural aminoglycosides (Figure 6, Supplementary Figure 6 and Supplementary Table 1). This loss is however rather limited (2-fold loss compared to paromomycin and neomycin) since, in contrast with the previous situation with the HIV DIS, no direct interaction should be lost according to known A site/neomycin crystal structure.[58]

Conclusions. We rationally designed and synthesized an aminoglycoside conjugate by replacing ring I with a thymine moiety, in order to form Watson−Crick hydrogen bonds with adenine 280 of the viral RNA. We showed that this conjugate **1** is able to bind DIS kissing-loops with an improved specificity compared to that of the parent compound neomycin, but only partial loss of affinity. In addition, conjugate **1** binds DIS from HIV-1 subtypes A, B, and F with a similar affinity, thus extending the specificity of binding to HIV-1 subtypes B RNA compared to neomycin. It was previously reported that neomycin inhibits up to 85% of HIV-1 production.[60] This effect might be due, at least partly, to the observed stabilization of the RNA dimer following drug binding to the DIS sequence.[18] The latter stabilization will induce excessive pauses and/or dissociation of the viral reverse transcriptase during proviral synthesis, thus interfering with virus production. Finally

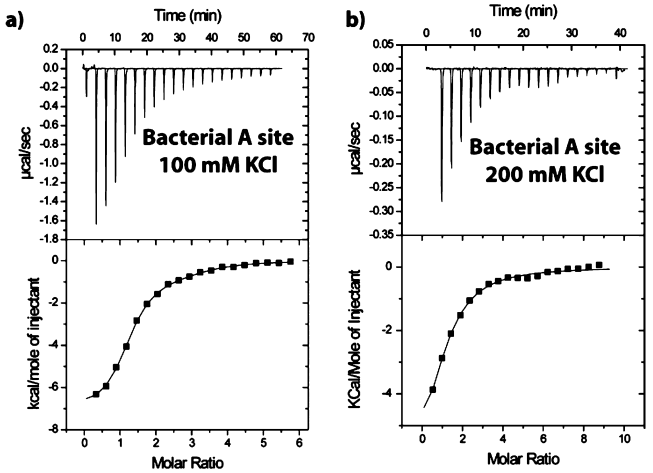

Figure 6. ITC profile for the titration of compound **1** in the bacterial A site in a solution containing either 100 mM KCl (a) or 200 mM KCl (b). Binding parameters are reported in Supplementary Table 1.

we showed that neomycin-thymine conjugate **1** binds the bacterial A site *in vitro* with a similar affinity than neomycin and

dx.doi.org/10.1021/cb400498n | ACS Chem. Biol. XXXX, XXX, XXX−XXX

paromomycin. It is therefore a potential new antibiotic with improved resistance against aminoglycoside-modifying enzymes, especially those affecting ring I like the neomycin 3′-phosphotransferase.[61] Work is in progress to evaluate the potential antiviral and antibacterial activity of conjugate **1**.

METHODS

Chemistry. Preparation of conjugate **1** is described in the Supporting Information.

RNA Sample Preparation. Chemically synthetized RNA sequences were purchased from Integrated DNA technologies or from Dharmacon. RNA were purified as described.[31] In short, RNA was loaded on a Nucleopac PA-100 column (Dionex) heated at 70 °C equilibrated in 4 M urea, 20 mM MES [2-(*N*-morpholino)-ethanesulfonic acid], pH 6.2 and eluted using a $NaClO_4$ gradient.

DIS kissing-loop complexes were obtained as follows: RNA was diluted to 2 μM concentration in water, heated at 90 °C for 5 min, and then cooled on ice for 5 min. As shown previously, this protocol essentially leads to the formation of DIS loop−loop dimers and prevents the formation of extended duplex dimers.[32,33] A similar protocol was performed for folding of TAR and SRL hairpins. The 22 base-pair RNA duplex was diluted to 60 μM in water, heated at 90 °C for 5 min, and then cooled at RT. This protocol was used in order to favor the formation of a duplex instead of hairpin monomers. All RNA samples were dialyzed against ITC buffer (25 mM Na cacodylate pH 7.0, 100 or 200 mM KCl, 2 mM $MgCl_2$) and adjusted to a final concentration of 10 to 60 μM.

Natural Aminoglycosides. Neomycin, paromomycin and lividomycin were purchased from Sigma-Aldrich and used without further purification. Aminoglycosides were dissolved into ITC buffer prior experiments.

Isothermal Titration Calorimetry (ITC). ITC measurements were performed on a MicroCal ITC_{200} (GE Healthcare) in ITC buffer containing 100 or 200 mM KCl. In a typical experiment, 20 injections of 2.0 μL aliquots of drug at 400 μM were injected (at 0.5 $\mu L\ s^{-1}$) into 203 μL of RNA at 12 μM in the sample cell. The delay between injections was 180 s. All ITC curves were analyzed using the software Origin (OriginLab) using either a one-site model (in absence of unspecific binding) or a two sets of sites model (in presence of unspecific binding). Standard free energies of binding (ΔG) were obtained using the equation

$$\Delta G = -RT \ln K_a$$

Entropic contributions were obtained from the relationship

$$\Delta G = \Delta H - T\Delta S$$

using standard free energy of binding determined previously and the binding enthalpies derived from fitted ITC data. In our experimental conditions, the product $K_a \times [RNA] \times N$, where N is the number of binding sites, lies in the 0.1−1000 range, allowing an accurate and simultaneous determination of binding parameters by ITC.[34] Because of a fast ligand-RNA binding, it was not possible to use our recently developed *kinITC* approach to derive kinetic parameters of binding in addition to thermodynamic data.[35]

Model Building. Modeling was carried out starting from the DIS kissing-loop/neomycin crystal structure[18] (PDB ID 2FCY) using the program O[36] followed by energy minimization using CNS.[37] The RNA was not fixed during the energy minimization.

ASSOCIATED CONTENT

Supporting Information

Supplementary methods, one table, and seven figures as described in the text. This material is available free of charge via the Internet at http://pubs.acs.org.

AUTHOR INFORMATION

Corresponding Authors

*E-mail: e.ennifar@ibmc-cnrs.unistra.fr.

*E-mail: f.vandelft@science.ru.nl.

Notes

The authors declare no competing financial interest.

ACKNOWLEDGMENTS

The authors thank T. Langer (Prestwick Chemical), V. Vidal (InPheno AG), and T. Klimkait (University of Basel) for fruitful and stimulating discussions. This work was supported by the Agence Nationale pour la Recherche (grant ANR-12-BS07-0007-03 “ClickEnARN”).

REFERENCES

(1) Paillart, J. C., Shehu-Xhilaga, M., Marquet, R., and Mak, J. (2004) Dimerization of retroviral RNA genomes: an inseparable pair. *Nat. Rev. Microbiol. 2*, 461−472.

(2) Laughrea, M., and Jetté, L. (1994) A 19-nucleotide sequence upstream of the 5′ major splice donor site is part of the dimerization domain of human immunodeficiency virus 1 genomic RNA. *Biochemistry 33*, 13464−13474.

(3) Skripkin, E., Paillart, J. C., Marquet, R., Ehresmann, B., and Ehresmann, C. (1994) Identification of the primary site of the Human Immunodeficiency Virus Type I RNA dimerization *in vitro*. *Proc. Natl. Acad. Sci. U.S.A. 91*, 4945−4949.

(4) Paillart, J.-C., Berthoux, L., Ottmann, M., Darlix, J.-L., Marquet, R., Ehresmann, C., and Ehresmann, B. (1996) A dual role of the dimerization initiation site of HIV-1 in genomic RNA packaging and proviral DNA synthesis. *J. Virol. 70*, 8348−8354.

(5) Shen, N., Jette, L., Liang, C., Wainberg, M. A., and Laughrea, M. (2000) Impact of human immunodeficiency virus type 1 RNA dimerization on viral infectivity and of stem-loop B on RNA dimerization and reverse transcription and dissociation of dimerization from packaging. *J. Virol. 74*, 5729−5735.

(6) Laughrea, M., and Jetté, L. (1996) Kissing-loop model of HIV-1 genome dimerization: HIV-1 RNA can assume alternative dimeric forms, and all sequences upstream or downstream of hairpin 248−271 are dispensable for dimer formation. *Biochemistry 35*, 1589−1598.

(7) Muriaux, D., Fossé, P., and Paoletti, J. (1996) A kissing complex together with a stable dimer is involved in the $HIV\text{-}1_{Lai}$ RNA dimerization process *in vitro*. *Biochemistry 35*, 5075−5082.

(8) Paillart, J. C., Skripkin, E., Ehresmann, B., Ehresmann, C., and Marquet, R. (1996) A loop-loop ″kissing″ complex is the essential part of the dimer linkage of genomic HIV-1 RNA. *Proc. Natl. Acad. Sci. U.S.A. 93*, 5572−5577.

(9) Takahashi, K. I., Baba, S., Chattopadhyay, P., Koyanagi, Y., Yamamoto, N., Takaku, H., and Kawai, G. (2000) Structural requirement for the two-step dimerization of human immunodeficiency virus type 1 genome. *RNA 6*, 96−102.

(10) Ennifar, E., and Dumas, P. (2006) Polymorphism of bulged-out residues in HIV-1 RNA DIS kissing complex and structure comparison with solution studies. *J. Mol. Biol. 356*, 771−782.

(11) Ennifar, E., Walter, P., and Dumas, P. (2010) Cation-dependent cleavage of the duplex form of the subtype-B HIV-1 RNA dimerization initiation site. *Nucleic Acids Res. 38*, 5807−5816.

(12) Ennifar, E., Walter, P., Ehresmann, B., Ehresmann, C., and Dumas, P. (2001) Crystal structures of coaxially stacked kissing complexes of the HIV-1 RNA dimerization initiation site. *Nat. Struct. Biol. 8*, 1064−1068.

(13) Ennifar, E., Yusupov, M., Walter, P., Marquet, R., Ehresmann, B., Ehresmann, C., and Dumas, P. (1999) The crystal structure of the dimerization initiation site of genomic HIV-1 RNA reveals an extended duplex with two adenine bulges. *Structure 7*, 1439−1449.

(14) Carter, A. P., Clemons, W. M., Brodersen, D. E., Morgan-Warren, R. J., Wimberly, B. T., and Ramakrishnan, V. (2000) Functional insights from the structure of the 30S ribosomal subunit and its interactions with antibiotics. *Nature 407*, 340−348.

(15) Vicens, Q., and Westhof, E. (2001) Crystal structure of paromomycin docked into the eubacterial ribosomal decoding A site. *Structure 9*, 647−658.
(16) Bernacchi, S., Freisz, S., Maechling, C., Spiess, B., Marquet, R., Dumas, P., and Ennifar, E. (2007) Aminoglycoside binding to the HIV-1 RNA dimerization initiation site: thermodynamics and effect on the kissing-loop to duplex conversion. *Nucleic Acids Res. 35*, 7128−7139.
(17) Ennifar, E., Paillart, J. C., Bernacchi, S., Walter, P., Pale, P., Decout, J. L., Marquet, R., and Dumas, P. (2007) A structure-based approach for targeting the HIV-1 genomic RNA dimerization initiation site. *Biochimie 89*, 1195−1203.
(18) Ennifar, E., Paillart, J. C., Bodlenner, A., Walter, P., Weibel, J. M., Aubertin, A. M., Pale, P., Dumas, P., and Marquet, R. (2006) Targeting the dimerization initiation site of HIV-1 RNA with aminoglycosides: from crystal to cell. *Nucleic Acids Res. 34*, 2328−2339.
(19) Ennifar, E., Paillart, J. C., Marquet, R., Ehresmann, B., Ehresmann, C., Dumas, P., and Walter, P. (2003) HIV-1 RNA dimerization initiation site is structurally similar to the ribosomal A site and binds aminoglycoside antibiotics. *J. Biol. Chem. 278*, 2723−2730.
(20) Tam, V. K., Kwong, D., and Tor, Y. (2007) Fluorescent HIV-1 Dimerization Initiation Site: design, properties, and use for ligand discovery. *J. Am. Chem. Soc. 129*, 3257−3266.
(21) Freisz, S., Lang, K., Micura, R., Dumas, P., and Ennifar, E. (2008) Binding of aminoglycoside antibiotics to the duplex form of the HIV-1 genomic RNA dimerization initiation site. *Angew. Chem., Int. Ed. 47*, 4110−4113.
(22) Borovinskaya, M. A., Pai, R. D., Zhang, W., Schuwirth, B. S., Holton, J. M., Hirokawa, G., Kaji, H., Kaji, A., and Cate, J. H. (2007) Structural basis for aminoglycoside inhibition of bacterial ribosome recycling. *Nat. Struct. Mol. Biol. 14*, 727−732.
(23) Hermann, T. (2007) Aminoglycoside antibiotics: old drugs and new therapeutic approaches. *Cell. Mol. Life Sci. 64*, 1841−1852.
(24) Mingeot-Leclercq, M. P., Glupczynski, Y., and Tulkens, P. M. (1999) Aminoglycosides: activity and resistance. *Antimicrob. Agents Chemother. 43*, 727−737.
(25) Houghton, J. L., Green, K. D., Chen, W., and Garneau-Tsodikova, S. (2010) The future of aminoglycosides: the end or renaissance? *ChemBioChem 11*, 880−902.
(26) Luedtke, N. W., Liu, Q., and Tor, Y. (2003) RNA-ligand interactions: affinity and specificity of aminoglycoside dimers and acridine conjugates to the HIV-1 Rev response element. *Biochemistry 42*, 11391−11403.
(27) Kumar, S., Kellish, P., Robinson, W. E., Jr., Wang, D., Appella, D. H., and Arya, D. P. (2012) Click dimers to target HIV TAR RNA conformation. *Biochemistry 51*, 2331−2347.
(28) Riguet, E., Desire, J., Boden, O., Ludwig, V., Gobel, M., Bailly, C., and Decout, J. L. (2005) Neamine dimers targeting the HIV-1 TAR RNA. *Bioorg. Med. Chem. Lett. 15*, 4651−4655.
(29) Bodlenner, A., Alix, A., Weibel, J. M., Pale, P., Ennifar, E., Paillart, J. C., Walter, P., Marquet, R., and Dumas, P. (2007) Synthesis of a neamine dimer targeting the dimerization initiation site of HIV-1 RNA. *Org. Lett. 9*, 4415−4418.
(30) Blount, K. F., and Tor, Y. (2006) A tale of two targets: differential RNA selectivity of nucleobase-aminoglycoside conjugates. *ChemBioChem 7*, 1612−1621.
(31) Ennifar, E., Walter, P., and Dumas, P. (2003) A crystallographic study of the binding of 13 metal ions to two related RNA duplexes. *Nucleic Acids Res. 31*, 2671−2682.
(32) Bernacchi, S., Ennifar, E., Toth, K., Walter, P., Langowski, J., and Dumas, P. (2005) Mechanism of hairpin-duplex conversion for the HIV-1 dimerization initiation site. *J. Biol. Chem. 280*, 40112−40121.
(33) Ennifar, E., Bernacchi, S., Wolff, P., and Dumas, P. (2007) Influence of C-5 halogenation of uridines on hairpin versus duplex RNA folding. *RNA 13*, 1445−1452.
(34) Velazquez Campoy, A., and Freire, E. (2005) ITC in the post-genomic era...? Priceless. *Biophys Chem 115*, 115−124.
(35) Burnouf, D., Ennifar, E., Guedich, S., Puffer, B., Hoffmann, G., Bec, G., Disdier, F., Baltzinger, M., and Dumas, P. (2011) kinITC: A new method for obtaining joint thermodynamic and kinetic data by isothermal titration calorimetry. *J. Am. Chem. Soc. 134*, 559−565.
(36) Jones, T. A. (1978) A graphic model building and refinement system for macromolecules. *J. Appl. Crystallogr. 11*, 268−272.
(37) Brunger, A. T., Adams, P. D., Clore, G. M., DeLano, W. L., Gros, P., Grosse-Kunstleve, R. W., Jiang, J. S., Kuszewski, J., Nilges, M., Pannu, N. S., Read, R. J., Rice, L. M., Simonson, T., and Warren, G. L. (1998) Crystallography & NMR system: A new software suite for macromolecular structure determination. *Acta Crystallogr., Sect. D: Biol. Crystallogr. 54*, 905−921.
(38) Greenberg, W. A., Priestley, E. S., Sears, P. S., Alper, P. B., Rosenbohm, C., Hendrix, M., Hung, S. C., and Wong, C. H. (1999) Design and synthesis of new aminoglycoside antibiotics containing neamine as an optimal core structure: correlation of antibiotic activity with in vitro inhibition of translation. *J. Am. Chem. Soc. 121*, 6527−6541.
(39) Wu, B., Yang, J., He, Y., and Swayze, E. E. (2002) Reexamination of neomycin B degradation: efficient preparation of its CD and D rings as protected glycosyl donors. *Org. Lett. 4*, 3455−3458.
(40) van den Broek, S. B., Gruijters, B. W., Rutjes, F. P., van Delft, F. L., and Blaauw, R. H. (2007) A short and scalable route to orthogonally O-protected 2-deoxystreptamine. *J. Org. Chem. 72*, 3577−3580.
(41) Corey, E. J., Hua, P. H., Pan, B. C., and Seitz, S. P. (1982) Total synthesis of aplasmomycin. *J. Am. Chem. Soc. 104*, 6818−6820.
(42) Pearlman, W. M. (1967) Noble metal hydroxides on carbon nonpyrophoric dry catalysts. *Tetrahedron Lett. 8*, 1663−1664.
(43) Faber, C., Sticht, H., Schweimer, K., and Rosch, P. (2000) Structural rearrangements of HIV-1 Tat-responsive RNA upon binding of neomycin B. *J. Biol. Chem. 275*, 20660−20666.
(44) Barbieri, C. M., and Pilch, D. S. (2006) Complete thermodynamic characterization of the multiple protonation equilibria of the aminoglycoside antibiotic paromomycin: a calorimetric and natural abundance 15N NMR study. *Biophys. J. 90*, 1338−1349.
(45) Francois, B., Russell, R. J., Murray, J. B., Aboul-ela, F., Masquida, B., Vicens, Q., and Westhof, E. (2005) Crystal structures of complexes between aminoglycosides and decoding A site oligonucleotides: role of the number of rings and positive charges in the specific binding leading to miscoding. *Nucleic Acids Res. 33*, 5677−5690.
(46) Han, Q., Zhao, Q., Fish, S., Simonsen, K. B., Vourloumis, D., Froelich, J. M., Wall, D., and Hermann, T. (2005) Molecular recognition by glycoside pseudo base pairs and triples in an apramycin-RNA complex. *Angew. Chem., Int. Ed. 44*, 2694−2700.
(47) Kaul, M., Barbieri, C. M., and Pilch, D. S. (2004) Fluorescence-based approach for detecting and characterizing antibiotic-induced conformational changes in ribosomal RNA: comparing aminoglycoside binding to prokaryotic and eukaryotic ribosomal RNA sequences. *J. Am. Chem. Soc. 126*, 3447−3453.
(48) Kaul, M., Barbieri, C. M., and Pilch, D. S. (2006) Aminoglycoside-induced reduction in nucleotide mobility at the ribosomal RNA A-site as a potentially key determinant of antibacterial activity. *J. Am. Chem. Soc. 128*, 1261−1271.
(49) Pilch, D. S., Kaul, M., Barbieri, C. M., and Kerrigan, J. E. (2003) Thermodynamics of aminoglycoside-rRNA recognition. *Biopolymers 70*, 58−79.
(50) Shandrick, S., Zhao, Q., Han, Q., Ayida, B. K., Takahashi, M., Winters, G. C., Simonsen, K. B., Vourloumis, D., and Hermann, T. (2004) Monitoring molecular recognition of the ribosomal decoding site. *Angew. Chem., Int. Ed. 43*, 3177−3182.
(51) Vicens, Q., and Westhof, E. (2002) Crystal structure of a complex between the aminoglycoside tobramycin and an oligonucleotide containing the ribosomal decoding a site. *Chem. Biol. 9*, 747−755.
(52) Vicens, Q., and Westhof, E. (2003) Crystal structure of Geneticin bound to a bacterial 16S ribosomal RNA A site oligonucleotide. *J. Mol. Biol. 326*, 1175−1188.

(53) Blount, K. F., Zhao, F., Hermann, T., and Tor, Y. (2005) Conformational constraint as a means for understanding RNA-aminoglycoside specificity. *J. Am. Chem. Soc. 127*, 9818−9829.
(54) Francois, B., Szychowski, J., Adhikari, S. S., Pachamuthu, K., Swayze, E. E., Griffey, R. H., Migawa, M. T., Westhof, E., and Hanessian, S. (2004) Antibacterial aminoglycosides with a modified mode of binding to the ribosomal-RNA decoding site. *Angew. Chem., Int. Ed. 43*, 6735−6738.
(55) Hanessian, S., Szychowski, J., Adhikari, S. S., Vasquez, G., Kandasamy, P., Swayze, E. E., Migawa, M. T., Ranken, R., Francois, B., Wirmer-Bartoschek, J., Kondo, J., and Westhof, E. (2007) Structure-based design, synthesis, and A-site rRNA cocrystal complexes of functionally novel aminoglycoside antibiotics: C2″ ether analogues of paromomycin. *J. Med. Chem. 50*, 2352−2369.
(56) Simonsen, K. B., Ayida, B. K., Vourloumis, D., Takahashi, M., Winters, G. C., Barluenga, S., Qamar, S., Shandrick, S., Zhao, Q., and Hermann, T. (2002) Novel paromamine derivatives exploring shallow-groove recognition of ribosomal-decoding-site RNA. *ChemBioChem 3*, 1223−1228.
(57) Vourloumis, D., Winters, G. C., Simonsen, K. B., Takahashi, M., Ayida, B. K., Shandrick, S., Zhao, Q., Han, Q., and Hermann, T. (2005) Aminoglycoside-hybrid ligands targeting the ribosomal decoding site. *ChemBioChem 6*, 58−65.
(58) Zhao, F., Zhao, Q., Blount, K. F., Han, Q., Tor, Y., and Hermann, T. (2005) Molecular recognition of RNA by neomycin and a restricted neomycin derivative. *Angew. Chem., Int. Ed. 44*, 5329−5334.
(59) Recht, M. I., Fourmy, D., Blanchard, S. C., Dahlquist, K. D., and Puglisi, J. D. (1996) RNA sequence determinants for aminoglycoside binding to an A-site rRNA model oligonucleotide. *J. Mol. Biol. 262*, 421−436.
(60) Zapp, M. L., Stern, S., and Green, M. R. (1993) Small molecules that selectively block RNA binding of HIV-1 Rev protein inhibit Rev function and viral production. *Cell 74*, 969−978.
(61) Pokrovskaya, V., Nudelman, I., Kandasamy, J., and Baasov, T. (2010) Aminoglycosides redesign strategies for improved antibiotics and compounds for treatment of human genetic diseases. *Methods Enzymol. 478*, 437−462.